HHS Public Access

Author manuscript

Nat Med. Author manuscript; available in PMC 2016 September 28.

Published in final edited form as:

Nat Med. 2016 May ; 22(5): 516–523. doi:10.1038/nm.4068.

Commensal microbiota affects ischemic stroke outcome by regulating intestinal γδT cells

Corinne Benakis[1,6], **David Brea**[1,6], **Silvia Caballero**[2,3], **Giuseppe Faraco**[1], **Jamie Moore**[1], **Michelle Murphy**[1], **Giulia Sita**[1], **Gianfranco Racchumi**[1], **Lilan Ling**[4], **Eric G. Pamer**[2,4,5], **Costantino Iadecola**[1], and **Josef Anrather**[1]

[1]Feil Family Brain and Mind Research Institute, Weill Cornell Medical College, New York, NY, USA

[2]Immunology Program and Infectious Disease Service, Memorial Sloan-Kettering Cancer Center, New York, NY, USA

[3]Immunology and Microbial Pathogenesis Program, Weill Cornell Graduate School of Medical Sciences, New York, NY, USA

[4]Lucille Castori Center for Microbes, Inflammation and Cancer, Memorial Sloan Kettering Cancer Center, New York, NY, USA

[5]Infectious Diseases Service, Department of Medicine, Memorial Sloan Kettering Cancer Center, New York, NY, USA

Abstract

Commensal gut bacteria impact the host immune system and can influence disease processes in several organs, including the brain. However, it remains unclear whether the microbiota has an impact on the outcome of acute brain injury. Here we show that antibiotic-induced alterations in the intestinal flora reduces ischemic brain injury in mice, an effect transmissible by fecal transplants. Intestinal dysbiosis alters immune homeostasis in the small intestine leading to an increase in regulatory T cells and a reduction in IL-17^{+} γδ T cells, through altered dendritic cell activity. Dysbiosis suppresses trafficking of effector T cells from the gut to the leptomeninges after stroke. Interleukin-10 (IL-10) and IL-17 are required for the neuroprotection afforded by intestinal dysbiosis. The findings reveal a previously unrecognized gut-brain axis and the impact of the intestinal flora and meningeal IL-17^{+} γδ T cells on ischemic injury.

Correspondence should be addressed to J.A. (; Email: joa2006@med.cornell.edu)

[6]These authors contributed equally to this work.

Author Contributions

C.B. and D.B. contributed to study design, performed, and/or contributed critically to all experiments, analyzed data, and contributed to writing of the manuscript. In some experiments, C.B. and D.B. were assisted by J.M., M.M., G.S. and G.R. G.F. performed EB extravasation experiments. E.G.P. and S.C. developed and provided the AC Res mouse model. L.L. performed r16S sequencing and together with E.G.P analyzed taxonomic data. C.I. contributed to study design and writing of the manuscript. J.A. formulated the original hypothesis, designed the study, analyzed data, and wrote the manuscript together with C.B., D.B and C.I. All authors read and approved the manuscript.

Note: Any Supplementary Information is available in the online version of the paper.

Introduction

Ischemic stroke is a highly prevalent disease with limited therapeutic options[1]. Inflammation is a key component in the pathophysiology of cerebral ischemia[2], and numerous experimental approaches have explored the therapeutic potential of immunomodulation[3]. However, our understanding of the interaction between resident brain cells and peripheral immune cells infiltrating the post-ischemic brain, and their role in tissue damage and repair, is still incomplete[3]. The peripheral immune system, involving both innate and adaptive immune cells, plays an essential role in the pathophysiology of stroke and contribute to secondary neurodegeneration by releasing neurotoxic factors including reactive oxygen and nitrogen species as well as exopeptidases[2].

The continuous interaction between the immune system and commensal microbes that populate the epithelial surfaces is essential for immune cell development, maintenance and function[4]. Intestinal commensal microbes, the most abundant symbiotic compartment in the body, have emerged as a potent regulator of lymphocyte populations, including regulatory T (T_{reg}) and γδ T cells, both of which are involved in cerebral ischemic injury[2]. γδ T cells, a major lymphocyte population with innate immune features, are located at epithelial surfaces including the intestine[5]. They can aggravate ischemic brain injury by secreting IL-17 and generating chemotactic signals for peripheral myeloid cells such as neutrophils and monocytes[6,7]. Although these studies suggested a causal involvement of IL-17$^+$ γδ T cells in ischemic brain injury, their origin and site of action have not been clearly elucidated. While effector T cells may contribute to focal ischemic injury, T_{reg} cells can contribute to neuroprotection by downregulating post-ischemic inflammation[8]. T_{reg} appear in the ischemic tissue after the acute phase and confer neuroprotection by secreting the anti-inflammatory cytokine IL-10, an effect thought to be antigen independent[9,10]. Despite exerting a protective effect, adoptively transferred T_{reg} do not enter the brain parenchyma in the acute phase of stroke[11], suggesting that T_{reg} exert their beneficial effect by modulating the peripheral immune system rather than acting on brain tissue directly[11]. Intestinal T_{reg} are indispensable for maintaining an anti-inflammatory environment in the gut by suppressing T_H17 cell differentiation[12,13] and γδ T cell proliferation[14]. In this study we investigated the effects of altered intestinal flora on the immune system and outcome after cerebral ischemia.

Results

Ischemic brain injury is reduced in mice with an altered intestinal flora

To modify the composition of the gut microbiota, we treated male C57BL/6 mice for 2 weeks with amoxicillin (β-lactam antibiotic) and clavulanic acid (β-lactamase inhibitor) (amoxicillin/clavulanate [AC] sensitive flora or AC Sens; Fig. 1a and Supplementary Fig. 1a). To control for off-target antibiotic effects, we established a mouse model that could be kept under antibiotic treatment without altering the intestinal flora. This was accomplished by co-housing experimental mice under AC treatment with seeder mice, which carry an AC-resistant gut microflora that is qualitatively similar to the one found in naïve animals (Supplementary Fig. 1b). Due to coprophagic behavior of mice, the resistant flora is successfully transmitted to naïve mice. Thus, AC-treated mice co-housed with these seeder animals acquire an AC-resistant microbiota (AC Res; Fig. 1a and Supplementary Fig. 1). AC

treatment reduced fecal bacterial copies over the first 3 days of treatment in AC Sens mice, but bacterial numbers recovered afterwards reflecting colonization with AC-insensitive bacterial species (Fig. 1b). No major changes in biomass were observed in AC Res mice, indicating a seamless transition from AC sensitive to AC-resistant flora. Phylogenetic analysis 2 weeks after the start of AC treatment revealed an alteration in the composition of the gut microbiota in AC Sens mice with an overall reduction in bacterial alpha-diversity and expansion of Proteobacteria and contraction of Firmicutes and Bacteroidetes (Fig. 1c).

Infarct volume was reduced by 60±6% in AC-treated mice with antibiotic-sensitive flora after transient middle cerebral artery occlusion (MCAO) compared to antibiotic-treated mice carrying a resistant flora (Fig. 1d). Sensorimotor function was better preserved in AC Sens than in AC Res mice 3 and 7 days post-ischemia (Fig 1e). This protective effect was not limited to this particular model of dysbiosis. Protection was also observed in mice treated with vancomycin, an antibiotic poorly absorbed by the gastrointestinal tract, even when treatment was discontinued 3 days prior to MCAO to eliminate possible systemic effects of antibiotic treatment (Supplementary Fig 2a,b). The vancomycin-induced changes in the composition of the intestinal flora were similar to those of AC Sens animals (Supplementary Fig. 2c), supporting the hypothesis that alterations in the intestinal flora result in neuroprotection. Body weight, rectal temperature, and intra-occlusion cerebral blood flow (CBF) did not differ among groups. Reperfusion CBF varied widely between groups, but, as reported in other models[15,16], had no relationship with the size of the infarct (Supplementary table 1 and Supplementary Fig. 3). To assess whether the protective effect of intestinal dysbiosis was due to alterations of the blood-brain barrier (BBB), which is altered in germ-free mice[17], we investigated BBB permeability. No difference in BBB permeability was detected between AC Res and AC Sens mice either at baseline or 6 hours after stroke, suggesting that alterations in BBB integrity did not account for the protection observed in AC Sens mice (Supplementary Fig. 4).

To assess whether these neuroprotective effects were directly mediated by the gut flora, a single fecal transplant was performed, transferring the flora from AC Res or AC Sens mice to mice pulse-treated with AC for 3 days (Fig. 1f). Mice underwent MCAO 14 days after transplant. Infarct volume (72 hours post MCAO) was reduced by 54±8% in mice that received fecal transplants from AC Sens mice compared to mice with AC Res transplants. We observed several commonalities in the microbial communities in antibiotic-treated mice and in mice receiving fecal transplants. Microbial diversity was reduced in mice receiving transplants from AC Sens donors (Supplementary Fig. 5a). As in antibiotic treated mice, Clostridiales and Bacteroidetes S24-7, the dominant bacterial classes in AC Res transplanted mice, were reduced in mice receiving AC Sens fecal transplants (Supplementary Fig. 5a). In place of Proteobacteria, we observed an expansion of Lachnospiraceae, Verrucomicrobiaceae and Anaeroplasmataceae. Despite the differences between antibiotic treated and transplanted mice, relative frequencies of several bacterial families, including Verrucomicrobiaceae, Prevotellaceae and Clostridiaceae, were identified as good predictors of infarct volume in both treatment paradigms by Random forest classification (Supplementary Fig. 5b).

Dysbiosis affects intestinal T_{reg} and IL-17$^+$ γδT cells

Next, we sought to elucidate the mechanisms of the protection exerted by altered gut flora 2 weeks after AC treatment. Ischemic stroke has an inflammatory component involving peripheral immune cells including lymphocytes[2]. Among these, T_{reg} and IL-17-producing γδ T cells (IL-17$^+$ γδ T) have been implicated in the mechanisms of ischemic injury[6,7,9,18]. The intestinal lamina propria (LP) and epithelium contain the largest population of T cells in the body, γδ T cells in particular, and the gut microbiota provide diverse signals for tuning the host immune system towards either an effector or regulatory phenotype[19,20]. Consequently, we investigated the effects of intestinal dysbiosis on T_{reg} and IL-17-producing T cells in the gut, blood, and secondary lymphoid organs. Flow cytometric analysis of intestinal immune cells revealed an increase in CD4$^+$FoxP3$^+$ T_{reg} and a reduction in IL-17$^+$ γδ T in the LP of the small intestine of AC Sens mice 2 weeks after treatment start, while IL-17-producing T helper cells (T_H17) were not affected (Fig. 2a,b). Similar changes were observed in intraepithelial T_{reg} cells but not in IL-17$^+$ γδ T cells. Independently of the treatment group, the frequency of IL-17$^+$ γδ T cells was lower in the intraepithelial lymphocytes (IELs) than in the LP (Supplementary Fig. 6a,b). Consistent with a selective regional effect of the altered microbiota on immune cell composition in the small intestine, the frequency of T_{reg} and IL-17$^+$ γδ T cells in the LP of the large intestine (Fig. 2b), peripheral blood, lymph nodes and spleen did not differ amongst groups (Supplementary Fig. 7). As in AC Sens mice, small intestine LP IL-17$^+$ γδ T cells were also reduced in vancomycin treated mice (Supplementary Fig. 6c). To assess the interdependence between the intestinal flora, gut immune cells and infarct volume, we determined these parameters in AC Res and AC Sens mice 1 week after start of antibiotic treatment. Whereas the microbial composition was different at 3 days after AC treatment (Supplementary Fig. 8a), intestinal microbial composition in AC Res and AC Sens mice at 1 week was similar to the one observed after 2 weeks (Supplementary Fig. 8b), indicating that the microbial community stabilized after 1 week, although bacterial numbers still expanded in AC Sens mice during the second week (Fig. 1b). Infarct volume, LP T_{reg} and LP IL-17$^+$ γδ T cells were not affected at 1 week (Supplementary Fig. 8c,d). Changes in intestinal T_{reg} and IL-17$^+$ γδ T cells are only apparent at two weeks when neuroprotection is also observed.

IL-17$^+$ γδ T cells accumulate in the meninges after stroke

Next, we addressed whether the immune response after stroke was altered in mice with intestinal dysbiosis. Flow cytometric analysis of brain immune cells revealed reduced infiltration of blood borne cells (CD45^{high}) at 2 and 3 days after reperfusion in AC Sens compared to AC Res mice (Fig. 3a). While all leukocyte types were reduced, neutrophils were more prominently diminished at day 2 (Fig. 3a). Because post-ischemic neutrophil infiltration contributes to brain injury[21,22], we sought to determine the expression of chemokines involved in neutrophil brain recruitment. We found that *Cxcl1* and *Cxcl2* mRNA expression were reduced in the brains of AC Sens mice compared to AC Res mice 24 hours after stroke (Fig. 3b). In line with reduced brain neutrophil infiltration we observed a trend for increased neutrophil numbers in the meninges of AC Sens mice 48 hours after stroke (Fig. 3c).

Because IL-17 is a major inducer of Cxcl1 and Cxcl2 chemokines[6,7], we examined the frequency of IL-17-producing cells in the brain after ischemia. Mice that carry GFP at the endogenous IL-17A locus (IL-17-GFP) were treated according to the AC Res or AC Sens protocol and underwent sham surgery or MCAO. Sixteen hours later, before the ischemic infarct is fully established, brains and meninges were processed for flow cytometric analysis. Only few γδ T cells were detected in the ischemic brain (data not shown) while the bulk of γδ T cells were found in the meninges. The frequency of meningeal γδ T cells was increased after stroke compared to sham mice (Fig. 3d) and IL-17 protein expression was higher in γδ T cells of AC Res mice after stroke compared to AC Sens mice which were not different from sham operated animals (Fig. 3d). We also observed T_{reg} in the meninges, but cell numbers were not different between AC Res and AC Sens mice (Supplementary Fig. 9). To determine the precise location of the cells within the meningeal layers, including the dura mater, arachnoid and pia mater, we examined immunofluorescent staining of intact skull sections of mice expressing GFP under control of the endogenous TCRδ locus. γδ T cells were localized to the leptomeninges 16 hours after MCAO (Fig. 3e). Some GFP^+ γδ T cell were also observed in the choroid plexus, a point of CNS entry for T cells[23], while the brain parenchyma was devoid of γδ T cells (data not shown).

Intestinal T cells traffic to the meninges after stroke

Next we assessed whether T cells that have acquired a regulatory or effector phenotype in the gut could traffic to cervical lymph nodes (cLN) and the meninges. Recent studies have shown bidirectional trafficking of leukocytes between the intestine and secondary lymphoid organs[24]. To this end we used mice (KikGR33) expressing the KikGR protein that stably photoconverts from green (G) to red (R) upon illumination with violet light[25]. We exposed the distal small intestine to violet light through a laparotomy, which resulted in efficient KikG to KikR conversion in gut resident but not in circulating immune cells (Supplementary Fig. 10). One week after photoconversion mice underwent MCAO. Gut, superficial and deep cLN, and meningeal immune cells were analyzed by flow cytometry 16 hours after stroke (Fig. 4a,b), a time point preceding leukocyte infiltration into the brain (Fig. 3a). The frequency of $KikR^+$ T cells was higher in the meninges than in superficial and deep cLN, suggesting gut-derived T cells preferentially home to the meninges after stroke (Fig. 4c). The frequency of $KikR^+$ B cells did not differ among tissues. As expected, the frequency of $KikR^+$ T cells was highest in the intestine (Fig. 4d). The percentage of intestinal $KikR^+$ T cells was lower than $KikR^+$ B cells, suggesting that T cells may exit the small intestine LP at higher rates than B cells as previously reported for the large intestine[24]. Virtually no KikR+ cell trafficking was observed in mice undergoing laparotomy without exposure to the light source (Fig. 4e).

Neuroprotection after dysbiosis depends on IL-17 and IL-10

Next, we tested whether suppression of IL-17 producing immune cells in AC Sens mice with the altered intestinal flora was sufficient to provide neuroprotection. IL-$17^{-/-}$ mice underwent either AC Res or AC Sens treatment protocols and subjected to MCAO 2 weeks later. Infarct volumes were similar between AC Res IL-$17^{-/-}$ and AC Sens IL-$17^{-/-}$ mice supporting an essential role for IL-17 in this model (Fig. 5a). Because our data indicates that small intestine T_{reg} cells are increased in AC Sens mice (Fig. 2a), we examined whether T_{reg}

cells are involved in the suppression of IL-17$^+$ γδ T cells in our model. Since IL-10 is involved in T_{reg} cell-mediated inhibition of γδ T effector cells[14], we utilized IL-10-deficient mice. Neuroprotection after stroke was not observed in AC-treated IL-10$^{-/-}$ mice (Fig. 5b) and the frequency of IL-17$^+$ γδ T in the small intestine LP did not differ between groups (Fig. 5c). These findings reveal a link between intestinal T_{reg} expansion and IL-10 and the reduction in IL-17$^+$ γδ T cells observed in AC Sens mice.

Dendritic cell reprogramming affects T cell differentiation

To address whether local immune cell interactions are modified by intestinal dysbiosis, we examined the impact of the gut flora on the capacity of intestinal antigen presenting cells to promote T_{reg} cells and IL-17$^+$ γδ T cell differentiation *in vitro*. Dendritic cells (DC) sustain immune homeostasis in the intestine by inducing T_{reg}26. We investigated whether altering the intestinal microflora impacts T cell differentiation by modulating the activity of intestinal DC. CD103$^+$ DCs originate in the intestinal lamina propria and migrate to the mesenteric LN (mLN) where they drive the differentiation of gut homing T_{reg}[26_28]. Consistent with a tolerogenic phenotype, we found that the percentage of CD11c$^+$CD11b$^+$CD103$^+$ DCs was higher in mLN isolated from AC Sens compared to AC Res mice (Fig. 6a). Then, we isolated DC from mLN in both AC Res and AC Sens mice and tested their respective abilities to induce T_{reg} and IL-17$^+$ γδ T cell differentiation. In co-cultures with CD4$^+$ T cells, DC from AC Sens mice were more efficient than DCs from AC Res mice in inducing T_{reg} cell differentiation (Fig. 6b). Upon co-culture with γδ T cells, DCs from AC Res mice were more effective at inducing IL-17$^+$ γδ T cells than DC from AC Sens mice (Fig. 6c), suggesting the commensal bacteria alters DCs.

IL-10 is required for T_{reg} mediated IL-17$^+$ γδ T suppression

Next we tested whether T_{reg} cells can suppress IL-17$^+$ γδ T differentiation *in vitro*. Increasing numbers of T_{reg} cells, generated by co-culturing CD4$^+$ T cells with DCs isolated from mLN of AC Sens or AC Res mice, were co-cultured with naïve γδ T cells. T_{reg} cells dose-dependently suppressed IL-17$^+$ γδ T differentiation and T_{reg} cells from co-cultures with AC Sens DCs were more efficient than T_{reg} cells obtained from co-cultures with AC Res DCs (Fig. 6d). To test if the suppression was mediated by IL-10, we compared T_{reg} cells generated by co-culturing AC Sens DCs with CD4$^+$ T cells isolated from wild-type (WT) or IL-10$^{-/-}$ mice. IL-10 deficiency reduced the capacity of T_{reg} cells to suppress IL-17$^+$ γδ T differentiation (Fig. 6d) even though T_{reg} numbers were comparable to WT cells (Fig. 6e).

Discussion

Our study describes a novel microbiota-gut-brain axis that is based on bacterial priming of intestinal DC leading to local T_{reg} expansion in the small intestine and effector IL-17$^+$ γδ T cell suppression. The data suggest that effector T cells traffic from the gut to the brain, where they localize in the leptomeninges and enhance ischemic neuroinflammation by secreting IL-17 resulting in increased chemokine production in the brain parenchyma and subsequent infiltration of cytotoxic immune cells including neutrophils (Fig. 6f).

Suggestive of an antigen-dependent imprinting, we found that DC isolated from mLN of AC Sens mice were more efficient in inducing T_{reg} than the DC isolated from mLN of AC Res mice. DC can directly sample intestinal content[29,30] and migrate to the mLN where they present antigens to induce T_{reg} polarization[26]. Consistent with the importance of this mechanism, we found that DC in mLN of AC Sens mice expressed higher levels of CD103, a marker of tolerogenic intestinal DC[26–28]. Compared to T_{reg} induction, the ability of DC from AC Sens mice to suppress IL-17$^+$ γδ T cell generation was less striking, suggesting that T_{reg} induction could be the main mechanism by which DC suppress IL-17$^+$ γδ T cells. Accordingly, we found that T_{reg} generated in co-cultures with AC Sens DC inhibited IL-17$^+$ γδ T differentiation more efficiently than T_{reg} generated by AC Res DC. In line with previous findings that identified IL-10 as a critical factor for T_{reg}-mediated of γδ T cell suppression[14], we found that IL-10$^{-/-}$ T_{reg} generated by co-culture with AC Sens DC were less efficient in suppressing IL-17$^+$ γδ T differentiation than WT T_{reg}. The suppressive activity of T_{reg} was not completely abolished, indicating that other mechanisms not affected by intestinal dysbiosis also play a role. This is to be expected, because IL-10 is only one of the possible mechanism by which T_{reg} suppress T cell proliferation[31]. Interestingly, the decrease of suppressive activity in IL-10$^{-/-}$ T_{reg} was similar to WT T_{reg} derived from co-cultures with AC Res DC, indicating that most of the dysbiosis-induced effects on IL-17$^+$ γδ T are IL-10 dependent. Accordingly, dysbiosis was unable to confer neuroprotection in IL-10$^{-/-}$ mice.

A new and unexpected finding of our study is the trafficking of intestinal T cells to the meninges. T cells are known to patrol the body including the brain where they enter through the choroid plexus into the cerebrospinal fluid[23] and probably drain through a recently described meningeal lymphatic system to the deep cervical lymph nodes[32]. Intestinal T cells have been found to traffic to extra-intestinal LN and spleen[24]. However, our data show that intestinal T cells preferentially accumulate in the meninges as opposed to cervical LN after stroke, possibly pointing to a directed gut-brain trafficking. Whereas T_{reg} were increased in the small intestine of mice with dysbiosis, T_{reg} in the meninges were not increased. While the evidence for a direct protective effect of brain-associated T_{reg} remains controversial[8,18,35,36], our data indicate that T_{reg} might affect stroke outcome independently of their presence in the brain, and through an intestinal mechanism involving IL-17$^+$ γδ T cell suppression. Our study also shows that the meninges function as a gatekeeper in post-ischemic inflammation. This is evidenced by the fact that γδ T cells did not enter the brain after stroke, but remained restricted to the leptomeninges where their numbers increased after stroke. Because inflammatory cells might enter the injured brain through extravasation from compromised meningeal vessels[37,38], meningeal IL-17$^+$ γδ T cells would be at a strategic location to control the trafficking to the brain parenchyma of monocytes and neutrophils – the main leukocyte populations found in the ischemic brain. In support of this interpretation, we found less IL-17$^+$ γδ T cells in the meninges after stroke in mice with intestinal dysbiosis, which was associated with reduced IL-17-responsive chemokine expression in the brain parenchyma. Although the role of γδ T cells as contributing factor to ischemic brain injury is not supported in all models[39], our study identifies IL-17$^+$ γδ T cells as the likely effector T cell regulated by intestinal dysbiosis. Because we found altered T_{reg} and IL-17$^+$ γδ T cells frequencies in the small intestine but not in the colon, peripheral

blood, spleen and LN of AC treated mice, alteration of bacteria residing in the small intestine could account for this effect. The bacterial specie(s) responsible for the gut immune changes underlying the protective effect of dysbiosis remain to be identified. AC treatment resulted in a profound alteration of intestinal microbiota characterized by a retraction of Clostridiaceae and S24-7 spp., a major family of Bacteroidetes, with concomitant expansion of Proteobacteria. Clostridiaceae and S24-7 Bacteroidetes were also reduced in mice receiving fecal transplants from AC Sens donors, raising the possibility that reduction in these bacterial families could be involved in the neuroprotection. Studies to identify the relevant bacterial species are underway.

IL-17 and γδ T cells have also been implicated in human stroke. Infiltration of γδ T cells and secretion of IL-17 have been documented in ischemic human brain tissue[7,40]. Circulating IL-17 is increased in stroke patients[41] and IL-17 expression in atherosclerotic lesions is associated with increased plaque vulnerability, a known risk factor for embolic stroke[42]. Given that several anti-IL-17 drugs are in clinical trials for a variety of inflammatory disorders (clinicaltrials.gov), use of such drugs in clinical stroke seams feasible once pharmacokinetic and safety data are available. Although no epidemiological data linking intestinal microbiota to stroke risk or stroke outcome are yet available, inflammatory bowel disease and Crohn's disease, which have been linked to altered gut flora and increased intestinal IL-17 production[19,43], have been identified as risk factors for stroke[44,45], suggesting that the microbiota-IL-17^{+} γδ T-brain axis identified in this study might also exist in humans.

In conclusion, our findings shed new light on poorly understood immune mechanisms that have a remarkable impact on brain injury, and have far reaching and translationally relevant implications for assessing cerebrovascular risk and predicting stroke severity.

ONLINE METHODS

Mice

All procedures were approved by the institutional animal care and use committee of Weill Cornell Medical College (Animal protocol number: 2012-0051). Wild-type C57BL/6, IL-10$^{-/-}$ (B6.129P2-Il10tm1Cgn/J), IL-17$^{-/-}$ (Il17atm1.1(icre)Stck/J), IL17-eGFP (C57BL/6-Il17atm1Bcgen/J), Trdc-eGFP (C57BL/6-Trdctm1Mal/J) and KikGR33 (Tg(CAG-KikGR)33Hadj/J) mice were purchased from Jackson Laboratories (JAX, Bar Harbor, Maine, USA). Genetically modified lines were bred in our facility. All mice were males on a C57BL/6 background except for KikGR33 mice, which were on a mixed C57BL/6-ICR background and for which male and female mice were used. All animal experiments were performed in accordance with the Animal Research: Reporting of *In Vivo* Experiments (ARRIVE) guidelines[46].

Mouse husbandry

Specific-pathogen-free (SPF) C57BL/6 mice (males; age = 6 weeks) were purchased from Jackson Laboratories and allowed to acclimatize in the Animal Facility for one week before being randomly assigned to experimental groups. The SPF status of the facility is

continuously monitored with sentinel animals by the Veterinary Service of Weill Cornell Medical College. JAX C57BL/6 mice do not harbor Segmented Filamentous Bacteria (SFB), a known inducer of T_H17 cells in mice[47]. JAX mice and mice derived from our housing facility used for this study tested negative for SFB by r16S sequencing of fecal pellets and by qPCR using SFB specific primers[48,49]. All mice were housed under a 12-hour light cycle in autoclaved microisolator cages with individual sterile air supply on autoclaved bedding and drinking water, and sterilized standard chow ad libitum. To minimize maternal effects on microbiota composition[50,51], mice from different litters were pooled before randomly assigning them to experimental groups.

Antibiotic treatment

C57BL/6 mice (males, 7 weeks) and IL-10$^{-/-}$, IL-17$^{-/-}$, IL-17-eGFP, Trdc-eGFP mice (males, 7–8 weeks) received 1 g/L of amoxicillin/clavulanic acid (AC, West-ward Pharmaceutical Corp. Eatontown, NJ) in autoclaved tap water for 1 or 2 weeks. Mice weighing less than 20 g at the beginning of the treatment were excluded from the study. All mice were housed in the same room and randomly allocated into two groups: AC-resistant (AC Res) mice co-housed for 2 weeks with an AC Res seeder mouse or AC-sensitive (AC Sens) mice. Additional mice were treated with water alone (H_2O) or vancomycin (0.5 g/L; Gold Biotechnology, St. Louis, MO) for 2 weeks. Administration of vancomycin was discontinued three days prior to middle cerebral artery occlusion (MCAO) to avoid off-target effects of antibiotics. Antibiotic water bottles were inverted every day and antibiotic solution was changed every 3–4 days together with cage bedding. To prevent bacterial cross-contamination, mouse handling and bi-weekly cage changes were performed by technicians wearing a clean gown and gloves in a ventilated hood.

Fecal microbial transplantation

Cecal contents were pooled from two donor mice. According to Caricilli *et al.* 2011 with slight modifications[52], cecal content was resuspended in PBS prepared in autoclaved tap water (2.5 ml per cecum), filtered using a strainer and stored at −80 °C until use. To facilitate colonization of the transplanted flora, recipient mice were pulse-treated for 3 days with AC prior to administration of 200 μl of cecal extract by oral gavage. Transplanted mice were kept on non-medicated water for 2 weeks after fecal transplantation until MCAO induction (Fig. 1f).

Middle cerebral artery occlusion

Transient focal cerebral ischemia was induced using the intraluminal filament model of MCAO, as described elsewhere[53]. Briefly, mice were anesthetized with 1.5–2% isoflurane, and rectal temperature was maintained at 37 ± 0.5 °C throughout surgery. A heat-blunted nylon suture (6/0) was inserted into the right external carotid artery and advanced until it obstructed the MCA together with the ligation of the common carotid artery for 35 min. Regional cerebral blood flow (CBF, bregma coordinates: 2 mm posterior, 5 mm lateral) was continuously recorded by transcranial laser Doppler flowmetry (Periflux System 5010; Perimed, King Park, NY) from the induction of ischemia until 30 min after reperfusion. We only included mice that had a residual CBF < 15% throughout the ischemic period and CBF recovery > 80% within 10 min of reperfusion. Following MCAO, mice were placed in

temperature controlled recovery cages for 2 hours to prevent post-surgery hypothermia. The order in which mice from different groups were subjected to MCAO was randomized. AC Sens mice cannot be blinded to the investigator because they exhibit an enlarged abdomen and stool pellets appear distinguishable from AC Res mice. Supplementary table 2 indicates the number of mice excluded and the percentage of survival after MCAO.

Measurement of infarct volume

Mice were euthanized 3 days after ischemia. Brains were frozen on dry ice and serially sectioned (600 μm intervals, 30 μm thick) for cresyl violet staining. Infarct volume, corrected for swelling[54], was quantified using an image analysis software (MCID; Imaging Research) by an investigator blinded to the treatment.

Behavioral Testing

Sensorimotor deficits were assessed 3 and 7 days after MCAO by the contact and removal adhesive tape test[55]. Mice were tested at the start of the dark phase of the circadian day-night cycle. Briefly, an adhesive tape 0.3 × 0.4 cm (Band-Aid®, flexible fabric, Johnson & Johnson) was placed on the dorsal aspect of both forepaws. Time duration of tape contact with the mouth and tape removal was scored on videos recorded over 180 s. At the beginning of each testing session mice were allowed to acclimate for 1 min in a glass cylinder covered by white paper. For training purpose, two days prior to MCAO induction, mice performed the test 4 times with 5–10 minutes rest cycles in the home cage between individual trials. Mice that were not able to remove the tape after training were excluded from the study (AC Res: $n = 2$; AC Sens: $n = 0$). Post-MCAO trials were conducted two times for 180 s each time to diminish stress effects related to handling. Results were expressed as contralateral contact and removal time. The sequence in which mice from different treatment groups were assessed was randomly assigned. AC Sens mice cannot be blinded to the investigator because they exhibit an enlarged abdomen and stool pellets appear distinguishable from AC Res mice.

Intact skull immunohistochemistry

Mice were anesthetized with isoflurane and perfused transcardially with ice-cold PBS followed by 4% PFA. After removing the mandibles, skin and muscles were carefully detached from the skull (http://www.nature.com/protocolexchange/protocols/3389). The skull decalcification was performed as previously described[56]. Coronal consecutive sections (10 μm) were cut using a cryostat set at a temperature of –23 °C. Skull sections were permeabilized with PBS and 0.5% Triton X-100, blocked with normal goat serum and incubated overnight at 4 °C with rabbit polyclonal anti-mouse pan-Laminin antibody (1:200; Z0097, DAKO) followed by Alexa-Fluor546-conjugated goat anti-rabbit secondary antibody (1:200; Molecular Probes, Invitrogen Corporation, Carlsbad, CA, USA). Sections were counterstained with TO-PRO-3 (Invitrogen) to visualize cell nuclei and observed by confocal laser microscopy (Leica SP5).

Brain blood brain barrier permeability by Evans Blue dye extravasation

Evans Blue (EB) dye (2%; 100 μl) was injected intravenously into the jugular vein of naïve AC Res and AC Sens mice or 5 hours after reperfusion in mice undergoing middle cerebral artery occlusion[57]. After one hour circulation, mice were perfused transcardially with ice-cold PBS. Brainstem and cerebellum were discarded and forebrains were separated into ipsilateral and contralateral hemispheres. Samples were weighed, frozen on dry ice and stored at –80 °C. Forebrains were homogenized in 500 μl of PBS, mixed with 500 μl of trichloroacetic acid and centrifuged. Supernatants were diluted 4 times with ethanol and samples were read in triplicate on a fluorescent plate reader (620 nm excitation, 680 nm emission). Standard curve was obtained using 0–500 ng/ml EB. Values were normalized for the weight difference by dividing each sample value (ng/ml) by the respective weight. Data are expressed as a ratio of EB dye in ipsilateral hemisphere/contralateral hemisphere (IH/CH).

Stool sample collection, DNA extraction

To avoid the confounding effects of co-housing on the diversity of the intestinal microbiota for each treatment group we collected samples from mice housed in different cages. Fresh stool pellets were collected and stored at –80 °C. Frozen stool samples (~100 mg) were placed in sterile polypropylene microvials (BioSpec Products) containing 1 ml InhibitEX Buffer (QIAGEN), 1 ml of 0.1 mm diameter zirconia/silica beads (BioSpec Products) and one 3.5 mm diameter glass bead (Biospec Products). Samples were homogenized for 2 min using a Mini-BeadBeater 16 (BioSpec Products). DNA was purified with the QIAamp Fast DNA Stool Mini Kit (QIAGEN) according to the manufacturer's instructions.

Quantification of r16S DNA copy numbers

r16S DNA sequences were amplified from stool DNA using 0.2 μM of the universal bacterial r16S gene primers 16S-V2-101F (5′–AGYGGCGIACGGGTGAGTAA–3′) and 16S-V2-361R (5′–CYIACTGCTGCCTCCCGTAG–3′) in conjunction with Maxima SYBR Green/ROX qPCR Master mix 2X (Thermo Scientific). Amplifications were performed on a Chromo 4 Detector (Bio-Rad, Hercules, CA) using a two-step cycling protocol consisting of: 50 °C for 2 min, 95 °C for 10 min, followed by 45 cycles of 95 °C for 15 s, 60 °C for 1 min. The standard curve was prepared using a plasmid containing an *E.coli* r16S V2 DNA fragment.

16S rRNA gene amplification and multiparallel sequencing

Amplicons of the V4-V5 16S rRNA region were amplified and sequenced using an Illumina MiSeq platform. For each sample, duplicate 50 μl PCR reactions were performed, each containing 50 ng of purified DNA, 0.2 mM dNTPs, 1.5 mM $MgCl_2$, 2.5 U Platinum Taq DNA polymerase, 2.5 μl of 10X PCR buffer, and 0.5 μM of each primer designed to amplify the V4-V5: 563F (5′–nnnnnnnn-NNNNNNNNNNNN-AYTGGGYDTAAAGNG–3′) and 926R (5′–nnnnnnnn-NNNNNNNNNNNN-CCGTCAATTYHTTTRAGT–3′). A unique 12-base Golay barcode (Ns) preceded the primers for sample identification, and one to eight additional nucleotides were placed in front of the barcode to offset the sequencing of the primers. Cycling conditions were 94 °C for 3 min, followed by 27 cycles of 94 °C for 50 s,

51 °C for 30 s, and 72 °C for 1 min. A condition of 72 °C for 5 min was used for the final elongation step. Replicate PCRs were pooled, and amplicons were purified using the QIAquick PCR Purification Kit (QIAGEN). PCR products were quantified and pooled at equimolar amounts prior to ligation of Illumina barcodes and adaptors according to Illumina TruSeq Sample Preparation protocol. The completed library was sequenced on an Illumina Miseq platform following the Illumina recommended procedures.

Sequence analysis

Sequences were analyzed using the mothur pipeline, version 1.33.3[58] as described previously[59]. Sequences with a distance-based similarity of 97% or greater were grouped into operational taxonomic units (OTU) using the furthest neighbor algorithm and classified using a modified in-house database containing sequences from GreenGenes 99 and retrieved 16S sequences from Genbank; OTU-based microbial diversity was estimated by calculating the Nonparametric Shannon diversity index (α-diversity). Sequence abundance profiles in each sample were used for downstream statistical and modeling analysis. A phylogenetic tree was inferred using Clearcut[60] on the 16S rRNA sequence alignment generated by mothur.

Quantitative determination of mRNA in brain tissue

A four millimeter slice of the ipsilateral forebrain was collected 24 h after middle cerebral artery occlusion and snap frozen in liquid nitrogen. The mRNA for chemokine (C-X-C motif) ligands *Cxcl1* and *Cxcl2* were examined by qRT-PCR as previously described[61]. Hypoxanthine-guanine phosphoribosyltransferase (*Hprt*) was used to normalize gene expression. Tissue was homogenized using a bead homogenizer (BioSpec Bartlesville, OK) with stainless steel beads in TRIzol® Reagent (Invitrogen Life Technologies, Grand Island, NY) and RNA was extracted according to the manufacturer's instructions. RNA samples were treated with Rnase free DnaseI (Roche, Indianapolis, IN) to remove DNA contamination. cDNA was produced from mRNA samples by using the RevertAid First Strand cDNA Synthesis Kit (Thermo Fisher Scientific, Waltham, MA). All primers were purchased from Invitrogen Life Technologies (Grand Island, NY). Primer sequences were as follows (Invitrogen): *Cxcl1*, 5′–GCGAAAAGAAGTGCAGAGAGA–3′ and 5′–AAACACAGCCTCCCACACAT–3′; *Cxcl2*, 5′–TGAACAAAGGCAAGGCTAACTG–3′ and 5′–GAGGCACATCAGGTACGATCC–3′ and *Hprt*, 5′–AGTGTTGGATACAGGCCAGAC–3′ and 5′–CGTGATTCAAATCCCTGAAGT–3′. qRT-PCR was conducted with 3 μl of cDNA (1:10 dilution), in duplicate 15 μl reactions using the Maxima SYBR Green/ROX qPCR Master Mix (2X) (Thermo Fisher Scientific, Waltham, MA). The reactions were incubated at 50 °C for 2 min and then at 95 °C for 10 min. A polymerase chain reaction cycling protocol consisting of 15 s at 95 °C and 1 min at 60 °C for 45 cycles was used for quantification. *Cxcl1* and *Cxcl2* relative expression levels were calculated by $2^{(-\Delta\Delta C(T))}$ method. Data were expressed as mean fold change in the ischemic hemisphere relative to naïve brain.

Cell isolation from lymphoid organs and blood

The spleen, mesenteric, axillary, inguinal deep and superficial cervical lymph nodes (LN) were isolated and placed on a pre-moistened 70 μm cell strainer. All lymphoid organs were

then gently homogenized with the end of a 1 ml syringe plunger. LN cells were eluted from the strainer with 10 ml PBS. For spleens, the strainer was washed with 10 ml erythrocytes lysis buffer (150 mM NH_4Cl, 1 mM $KHCO_3$, 0.1 mM EDTA; pH 7.2) eluted cells were incubated for 5 min at room temperature and washed with 40 ml PBS. Blood was drained from the submandibular vein into tubes containing sodium heparin, incubated for 5 min at room temperature with erythrocytes lysis buffer followed by addition of 10 ml of HBSS/10mM HEPES. Cell suspensions were centrifuged at 500 *g* for 7 min and subsequently stained for flow cytometric analysis, or stimulated *in vitro* for analysis of intracellular cytokines.

Cell isolation from mesenteric lymph nodes for dendritic cells analysis

For dendritic cell analysis, mesenteric lymph nodes were isolated and digested with 5 ml HBSS/10mM HEPES containing 5% FBS and 0.2 mg/ml collagenase D (Sigma). Tissue was digested at 37 °C for 20 min with constant agitation (250 rpm), then vigorously vortexed for 20 s. The resulting cell suspension was filtered through a 40 μm nylon cell strainer and washed with 10 ml PBS. Cell suspensions were centrifuged at 500 *g* for 7 min and subsequently stained for flow cytometric analysis.

Isolation of intestinal intraepithelial lymphocytes (IELs) and lamina propria mononuclear cells (LPMCs)

Mice were sacrificed by pentobarbital overdose (Sigma; 200 mg/kg; i.p.). Small and large intestines were removed and separated. Peyer's patches were excised and intestines were cleaned of mesenteric fat and intestinal contents. Then intestines were opened longitudinally, washed with PBS, cut into ~1 cm pieces and placed into 20 ml of HBSS/10 mM HEPES, 8% FBS, 4 mM EDTA, 0.5 mM dithiothreitol. Tissue pieces were washed three times in a shaking incubator set at 250 rpm and 37 °C for 20 min. After each round, tissue suspension was vortexed for 20 s and the supernatant containing IELs was collected. Supernatants were combined and filtered first over 0.3 g of pre-moistened nylon wool placed in a 10 ml syringe and then over a 70 μm strainer. Remaining tissue pieces were washed with Ca^{++}/Mg^{++}-PBS to remove EDTA, minced thoroughly, and placed into 5 ml HBSS/10 mM HEPES containing 5% FBS and 0.2 mg/ml collagenase D (Sigma). Tissue was digested at 37 °C for 20 min with constant agitation (250 rpm), then vigorously vortexed for 20 s. The resulting cell suspension containing LPMCs was filtered through a 40 μm nylon cell strainer and washed with 10 ml PBS. IEL and LPMC cell suspensions were collected at 500 *g* for 10 min at 4 °C. Cell pellets were resuspended in 8 ml 44% Percoll (GE healthcare, #57-0891-01) and overlaid over 5 ml of 67% Percoll. Gradients were centrifuged at 500 *g* for 20 min at 4 °C and cells at the interface were collected and washed with 10 ml PBS. Cells were stained for flow cytometric analysis or used for *in vitro* stimulation.

Isolation of brain leukocytes

Isolation of brain leukocytes was performed according to Pino *et al.*[62]. Briefly, mice were anesthetized with pentobarbital and transcardially perfused with 20 ml cold PBS. Brains were removed, olfactory bulbs, cerebellum excised and hemispheres separated. One hemisphere was placed in a douncer containing 3 ml RPMI-1640 with phenol red and gently homogenized. Then 4 ml of RPMI and 3 ml of Percoll 100% (final concentration 30%

Percoll) were added and overlaid over 2 ml of 70% Percoll. Gradients were centrifuged at 500 *g*, for 30 min at 18 °C. Cells were recovered from the interface, washed twice with PBS and either stained for flow cytometric analysis or used for *in vitro* stimulation.

Meningeal cell isolation

Mice were anesthetized with pentobarbital and transcardially perfused with 20 ml cold PBS. The upper portion of the skull was separated from the brain and meninges were recovered from the interior of the skull bones under a dissection microscope. Meninges were placed on the surface of a pre-moistened 70 μm cell strainer. Tissue was gently homogenized with the end of a 1 ml syringe plunger, washed with 10 ml PBS and centrifuged at 500 *g* for 7 min. Cells were either stained for flow cytometric analysis or stimulated *in vitro* for analysis of intracellular cytokines.

Flow cytometry analysis

For surface marker analysis, cell suspensions were adjusted to a density of $1' 10^6$ cells in 50 μl FACS buffer (2% FBS, 0.05% NaN_3 in PBS). Nonspecific binding was blocked by incubation for 10 min at 4 °C with anti-CD16/CD32 antibody (Biolegend, clone 93, 5 ng/μL) antibody and stained with the appropriate antibodies for 15 min at 4 °C. The following antibodies were used for extracellular staining: CD45 (clone 30F-11, 0.5 ng/μL), CD4 (clone RM4-5, 0.5 ng/μL), TCR-β (clone H57-597, 4 ng/μL), TCR-γδ (clone GL3, 4 ng/μL), CD11b (clone M1/70, 0.6 ng/μL), Ly6G (clone 1A8, 2 ng/μL), CD11c (clone N418, 2 ng/μL), NK1.1 (clone PK136, 0.32 ng/μL), CD19 (clone 6D5, 0.6 ng/μL), CD103 (clone 2E7, 1.5 ng/μL), F4/80 (clone BM8, 0.5 ng/μL), B220 (clone RA3-6B2, 0.32 ng/μL), CD3ε (clone 145-2C11, 2 ng/μL) from Biolegend. For intracellular staining, cells were first stained for surface markers as detailed above, fixed and permeabilized using Fixation and Permeabilization Buffers from eBiosciences following the manufacturer's instructions. Briefly, cells were fixed for 30 min at 4 °C, washed with permeabilization buffer and incubated for 30 min with the appropriate antibodies in permeabilization buffer at 4 °C. The following antibodies were used: FoxP3 (clone FJK-16s, 0.5 ng/μL) and IL-17A (clone eBio17B7, 1 ng/μL) from eBiosciences. Cells were washed with FACS buffer, resuspended in 200 μl of FACS buffer and analyzed with a MACSQuant10 cytometer (Myltenyi Biotech). Analysis was performed with FlowJo software (Vers. 10, Tree Star). Gates were validated by TO-PRO-3 and fluorescein-diacetate labeling to identify dead and live cells, respectively. Isotype controls, single antibody-stained samples and Fluorescence Minus One controls were used to establish compensation and gating parameters[63]. Samples were acquired and analyzed by an investigator blinded to the treatment groups.

In vitro stimulation for intracellular IL-17 expression analysis

For IL-17 analysis, we used either IL-17-GFP reporter mice or anti-IL-17 antibodies in wild-type mice. Cells pooled from 2 animals were resuspended in RPMI-1640 containing 10% FBS, 100 ng/ml phorbol 12-myristate 13-acetate (PMA) and 1 μg/ml ionomycin. Brefeldin (3 μg/ml, Sigma) was added for intracellular IL-17 staining. Cells were incubated for 4 h at 37 °C, and then washed and stained as indicated above for flow cytometric analysis.

Photoconversion of KikGR mice

Mice were anesthetized with 2.5% isoflurane (vol/vol), delivered in 2 L/min of 30% O_2 and 70% N_2O, and maintained at 37 °C throughout the procedure. Photoconversion was performed with a defocused (1.5 cm beam diameter) violet laser source (405 nm, peak power 4.5 mW, ThorLabs) essentially as described[24]. Briefly, mice were placed in a supine position and covered with an aluminum foil blanket. A 3 cm incision was made into the abdominal wall, exposing the distal part of the small intestine. The exposed gut segment (~6 cm) was illuminated for 20 min through an opening in the aluminum foil covering the animal. Intestinal tissue was kept hydrated by applying saline throughout the procedure. The intestine was returned to the abdominal cavity and the peritoneum and skin were sutured closed. 7 days after photoconversion mice were subjected to MCAO and 16 h later mice were anesthetized with pentobarbital intraperitoneally and transcardially perfused with 20 ml cold PBS. Deep and superficial LN, meninges and LPMC from small intestine were extracted and prepared as previously indicated for flow cytometric analysis (three animals were pooled) and percentage of photoconverted red cells ($KikR^+$) was analyzed in B and T cell populations.

Isolation of dendritic cells, $CD4^+$ and γδ T cells

Mice were sacrificed by pentobarbital overdose. Mesenteric lymph nodes (LN) were extracted and digested for 20 min at 37 °C with collagenase type IV (0.2 mg/ml; Sigma) in HBSS/10 mM HEPES with 5% of FBS. Cell suspension was enriched for $CD11c^+$ cells by positive selection on MS MACS Columns (Miltenyi Biotec) using an anti-CD11c-PE antibody (clone N418) and anti-PE microbeads (purity > 75%). CD4 T cells were isolated by incubating splenocytes with the following biotinylated antibodies: CD8a (clone 53–6.7, 187 ng/μL), B220 (clone RA3-6B2, 47 ng/μL), CD49b (clone Hma2, 94 ng/μL), CD11b (clone M1/70, 94 ng/μL) and TER119 (clone TER119, 38 ng/μL). This was followed by anti-biotin microbeads and negative enrichment with LS MACS columns according to the manufacturer's instructions (Miltenyi Biotec). Purity was consistently greater than 95%. γδ T cells were isolated from the spleen and LNs of Trdc-eGFP mice. Three to four mice were pooled for each γδ T isolation. Splenocytes and LN cells were prepared as described above and incubated with the following biotinylated antibodies: TCR-β (clone H57-597, 187 ng/μL), B220 (clone RA3-6B2, 47 ng/μL), CD49b (clone Hma2, 94 ng/μL), CD11b (clone M1/70, 94 ng/μL) and TER119 (clone TER119, 38 ng/μL). This was followed by anti-biotin microbeads and negative selection with LS MACS columns according to the manufacturer's specifications (Miltenyi Biotec) (purity > 65%).

In vitro induction of regulatory T cells

Mesenteric lymph node dendritic cells (DC) isolated from AC Res and AC Sens mice were cultured with $CD4^+$ cells from naïve mice ($2.5 \prime 10^4$ DC and $2.5 \prime 10^4$ $CD4^+$ cells per well in 96 well-plates), in RPMI 1640 with 10% FBS, 2 mM L-glutamine, 30 μM β-mercaptoethanol, non-essential amino acids (NEAAs), 1 mM sodium pyruvate, penicillin/streptomycin together with 1 μg/ml anti-CD3 (clone 17A2) and 100 U/ml of IL-2 (Biolegend) for 3 days, either with or without TGF-β1 (1 ng/ml, PreproTech). Cells were washed with FACS buffer, blocked with CD16/32 antibodies for 10 min at 4 °C and stained

with CD45 and TCR-β antibodies for 15 min at 4 °C. Cells were fixed/permeabilized for 30 min at 4 °C and then intracellularly stained with FoxP3 antibody for 30 min at 4 °C for flow cytometric analysis. Percentage of $FoxP3^+$ cells in the $CD4^+$ cell population ($CD45^+TCR\text{-}\beta^+CD4^+$) was calculated.

In vitro induction of IL-17-producing γδ T cells

Mesenteric lymph node dendritic cells (DC) isolated from AC Res and AC Sens mice were cultured with γδ T cells from naive Trdc-eGFP mice for three days ($2.5 \prime 10^4$ DC and $2.5 \prime 10^4$ γδ T cells per well in 96 well-plates precoated with 10 μg/ml of TCR-γδ antibody: clone GL4) in RPMI-1640 with 10% FBS, 2 mM L-glutamine, 30 μM β-mercaptoethanol, NEAAs, 1 mM sodium pyruvate and penicillin/streptomycin. Then cells were washed with fresh medium and resuspended in RPMI-1640 containing 10% FBS, 100 ng/ml PMA, 1 μg/ml ionomycin and brefeldin (3 μg/ml, Sigma) and incubated for 4 h at 37 °C, and then washed and stained as previously indicated for flow cytometric analysis and percentage of $IL\text{-}17^+$ cells in the γδ T cell population was calculated.

In vitro suppression of IL-17-producing γδ T cells

T_{reg} were induced as described above by co-culturing $CD4^+$ cells from naïve wild-type or $IL\text{-}10^{-/-}$ mice with AC Res or AC Sens DC. At day 3 of culture, cells were collected and $CD4^+$ cells were isolated by negative selection. Cells were co-cultured at different ratios (0:1, 1:8, 1:4, 1:2, 1:1) with γδ T cells (2.5×10^4 cells) freshly isolated from naïve Trdc-eGFP mice in 96 well-plates precoated with 10 μg/ml of TCR-γδ antibody (clone GL4) in RPMI-1640 with 10% FBS, 2 mM L-glutamine, 30 μM β-mercaptoethanol, NEAAs, 1 mM sodium pyruvate and penicillin/streptomycin for 4 days. Then cells were washed and re-stimulated as described above. Cells were washed with FACS buffer, blocked with CD16/32 antibodies and stained with CD45 and TCR-β. Cells were fixed and permeabilized for 30 min and intracellularly stained with anti-IL-17 antibody for 30 min at 4 °C for flow cytometric analysis. Number of $IL\text{-}17^+$ cells in the γδ T cell population ($CD45^+TCR\text{-}\beta^-TCR\text{-}\delta\text{-}GFP^+$) was calculated and normalized to $IL\text{-}17^+$ γδ T cell numbers in the control group (ratio T_{reg}:γδ T cells 0:1).

Supplementary Material

Refer to Web version on PubMed Central for supplementary material.

Acknowledgments

J.A. is the recipient of the Finbar and Marianne Kenny Research Scholarship. Parts of the study were supported by NIH grant NS081179 (J.A.), the Feil Family Foundation, the Swiss National Science Foundation and the Swiss Foundation for Grants in Biology and Medicine (SFGBM P3SMP3 148367; C.B.). We thank A-K Hadjantonakis for helpful discussion on the use of KikGR33 mice.

References

1. Henninger N, Kumar R, Fisher M. Acute ischemic stroke therapy. Expert Rev Cardiovasc Ther. 2010; 8:1389–1398. [PubMed: 20936925]
2. Iadecola C, Anrather J. The immunology of stroke: from mechanisms to translation. Nat Med. 2011; 17:796–808. [PubMed: 21738161]

3. Macrez R, et al. Stroke and the immune system: from pathophysiology to new therapeutic strategies. Lancet Neurol. 2011; 10:471–480. [PubMed: 21511199]
4. Mazmanian SK, Liu CH, Tzianabos AO, Kasper DL. An immunomodulatory molecule of symbiotic bacteria directs maturation of the host immune system. Cell. 2005; 122:107–118. [PubMed: 16009137]
5. Prinz I, Silva-Santos B, Pennington DJ. Functional development of γδ T cells. Eur J Immunol. 2013; 43:1988–1994. [PubMed: 23928962]
6. Shichita T, et al. Pivotal role of cerebral interleukin-17-producing γδT cells in the delayed phase of ischemic brain injury. Nat Med. 2009; 15:946–950. [PubMed: 19648929]
7. Gelderblom M, et al. Neutralization of the IL-17 axis diminishes neutrophil invasion and protects from ischemic stroke. Blood. 2012; 120:3793–3802. [PubMed: 22976954]
8. Liesz A, Hu X, Kleinschnitz C, Offner H. Functional role of regulatory lymphocytes in stroke: facts and controversies. Stroke. 2015; 46:1422–1430. [PubMed: 25791715]
9. Liesz A, et al. Regulatory T cells are key cerebroprotective immunomodulators in acute experimental stroke. Nat Med. 2009; 15:192–199. [PubMed: 19169263]
10. Stubbe T, et al. Regulatory T cells accumulate and proliferate in the ischemic hemisphere for up to 30 days after MCAO. Journal of Cerebral Blood Flow & Metabolism. 2013; 33:37–47. [PubMed: 22968321]
11. Li P, et al. Adoptive regulatory T_cell therapy protects against cerebral ischemia. Ann Neurol. 2013; 74:458–471. [PubMed: 23674483]
12. Chaudhry A, et al. CD4+ regulatory T cells control TH17 responses in a Stat3-dependent manner. Science. 2009; 326:986–991. [PubMed: 19797626]
13. Huber S, et al. Th17 cells express interleukin-10 receptor and are controlled by Foxp3 and Foxp3+ regulatory CD4+ T cells in an interleukin-10-dependent manner. Immunity. 2011; 34:554–565. [PubMed: 21511184]
14. Park SG, et al. T regulatory cells maintain intestinal homeostasis by suppressing γδ T cells. Immunity. 2010; 33:791–803. [PubMed: 21074460]
15. Cho S, et al. The class B scavenger receptor CD36 mediates free radical production and tissue injury in cerebral ischemia. J Neurosci. 2005; 25:2504–2512. [PubMed: 15758158]
16. Kunz A, et al. Neurovascular protection by ischemic tolerance: role of nitric oxide and reactive oxygen species. J Neurosci. 2007; 27:7083–7093. [PubMed: 17611261]
17. Braniste V, et al. The gut microbiota influences blood-brain barrier permeability in mice. Sci Transl Med. 2014; 6:263ra158–263ra158.
18. Hu X, Li P, Chen J. Pro: Regulatory T cells are protective in ischemic stroke. Stroke. 2013; 44:e85–6. [PubMed: 23821231]
19. Round JL, Mazmanian SK. The gut microbiota shapes intestinal immune responses during health and disease. Nat Rev Immunol. 2009; 9:313–323. [PubMed: 19343057]
20. Nishio J, Honda K. Immunoregulation by the gut microbiota. Cell Mol Life Sci. 2012; 69:3635–3650. [PubMed: 22527722]
21. Justicia C, et al. Neutrophil infiltration increases matrix metalloproteinase-9 in the ischemic brain after occlusion/reperfusion of the middle cerebral artery in rats. J Cereb Blood Flow Metab. 2003; 23:1430–1440. [PubMed: 14663338]
22. Stowe AM, et al. Neutrophil elastase and neurovascular injury following focal stroke and reperfusion. Neurobiol Dis. 2009; 35:82–90. [PubMed: 19393318]
23. Engelhardt B, Ransohoff RM. The ins and outs of T-lymphocyte trafficking to the CNS: anatomical sites and molecular mechanisms. Trends in Immunology. 2005; 26:485–495. [PubMed: 16039904]
24. Morton AM, et al. Endoscopic photoconversion reveals unexpectedly broad leukocyte trafficking to and from the gut. Proc Natl Acad Sci USA. 2014; 111:6696–6701. [PubMed: 24753589]
25. Nowotschin S, Hadjantonakis AK. Use of KikGR a photoconvertible green-to-red fluorescent protein for cell labeling and lineage analysis in ES cells and mouse embryos. BMC Dev Biol. 2009; 9:49. [PubMed: 19740427]

26. Coombes JL, et al. A functionally specialized population of mucosal CD103+ DCs induces Foxp3+ regulatory T cells via a TGF-beta and retinoic acid-dependent mechanism. J Exp Med. 2007; 204:1757–1764. [PubMed: 17620361]
27. Scott CL, Aumeunier AM, Mowat AM. Intestinal CD103+ dendritic cells: master regulators of tolerance? Trends in Immunology. 2011; 32:412–419. [PubMed: 21816673]
28. Ochoa-Repáraz J, et al. A polysaccharide from the human commensal Bacteroides fragilis protects against CNS demyelinating disease. Mucosal Immunol. 2010; 3:487–495. [PubMed: 20531465]
29. Rescigno M, et al. Dendritic cells express tight junction proteins and penetrate gut epithelial monolayers to sample bacteria. Nat Immunol. 2001; 2:361–367. [PubMed: 11276208]
30. Niess JH, et al. CX3CR1-mediated dendritic cell access to the intestinal lumen and bacterial clearance. Science. 2005; 307:254–258. [PubMed: 15653504]
31. Josefowicz SZ, Lu LF, Rudensky AY. Regulatory T cells: mechanisms of differentiation and function. Annu Rev Immunol. 2012; 30:531–564. [PubMed: 22224781]
32. Louveau A, et al. Structural and functional features of central nervous system lymphatic vessels. Nature. 2015; 523:337–341. [PubMed: 26030524]
33. Steffen BJ, Breier G, Butcher EC, Schulz M, Engelhardt B. ICAM-1, VCAM-1, and MAdCAM-1 are expressed on choroid plexus epithelium but not endothelium and mediate binding of lymphocytes in vitro. Am J Pathol. 1996; 148:1819–1838. [PubMed: 8669469]
34. Gorfu G, Rivera-Nieves J, Ley K. Role of beta7 integrins in intestinal lymphocyte homing and retention. 2009; 9:836–850.
35. Kleinschnitz C, Wiendl H. Con: Regulatory T cells are protective in ischemic stroke. Stroke. 2013; 44:e87–8. [PubMed: 23821227]
36. Kleinschnitz C, et al. Regulatory T cells are strong promoters of acute ischemic stroke in mice by inducing dysfunction of the cerebral microvasculature. Blood. 2013; 121:679–691. [PubMed: 23160472]
37. Roth TL, et al. Transcranial amelioration of inflammation and cell death after brain injury. Nature. 2014; 505:223–228. [PubMed: 24317693]
38. Pérez-de Puig I, et al. Neutrophil recruitment to the brain in mouse and human ischemic stroke. Acta Neuropathol (Berl). 2015; 129:239–257. [PubMed: 25548073]
39. Kleinschnitz C, et al. Early detrimental T-cell effects in experimental cerebral ischemia are neither related to adaptive immunity nor thrombus formation. Blood. 2010; 115:3835–3842. [PubMed: 20215643]
40. Li GZ, et al. Expression of interleukin-17 in ischemic brain tissue. Scand J Immunol. 2005; 62:481–486. [PubMed: 16305645]
41. Kostulas N, Pelidou SH, Kivisäkk P, Kostulas V, Link H. Increased IL-1beta, IL-8, and IL-17 mRNA expression in blood mononuclear cells observed in a prospective ischemic stroke study. Stroke. 1999; 30:2174–2179. [PubMed: 10512924]
42. Erbel C, et al. Expression of IL-17A in human atherosclerotic lesions is associated with increased inflammation and plaque vulnerability. Basic Res Cardiol. 2011; 106:125–134. [PubMed: 21116822]
43. Abraham C, Cho J. Interleukin-23/Th17 pathways and inflammatory bowel disease. Inflamm Bowel Dis. 2009; 15:1090–1100. [PubMed: 19253307]
44. Keller JJ, et al. Increased risk of stroke among patients with Crohn's disease: a population-based matched cohort study. Int J Colorectal Dis. 2015; 30:645–653. [PubMed: 25608496]
45. Singh S, Kullo IJ, Pardi DS, Loftus EV. Epidemiology, risk factors and management of cardiovascular diseases in IBD. Nat Rev Gastroenterol Hepatol. 2015; 12:26–35. [PubMed: 25446727]
46. Kilkenny C, et al. Animal research: reporting in vivo experiments--the ARRIVE guidelines. Journal of Cerebral Blood Flow & Metabolism. 2011; 31:991–993. [PubMed: 21206507]
47. Ivanov II, et al. Induction of intestinal Th17 cells by segmented filamentous bacteria. Cell. 2009; 139:485–498. [PubMed: 19836068]

48. Snel J, et al. Comparison of 16S rRNA sequences of segmented filamentous bacteria isolated from mice, rats, and chickens and proposal of “Candidatus Arthromitus”. Int J Syst Bacteriol. 1995; 45:780–782. [PubMed: 7547299]
49. Barman M, et al. Enteric salmonellosis disrupts the microbial ecology of the murine gastrointestinal tract. Infect Immun. 2008; 76:907–915. [PubMed: 18160481]
50. Benson AK, et al. Individuality in gut microbiota composition is a complex polygenic trait shaped by multiple environmental and host genetic factors. Proc Natl Acad Sci USA. 2010; 107:18933–18938. [PubMed: 20937875]
51. Ubeda C, et al. Familial transmission rather than defective innate immunity shapes the distinct intestinal microbiota of TLR-deficient mice. J Exp Med. 2012; 209:1445–1456. [PubMed: 22826298]
52. Caricilli AM, et al. Gut microbiota is a key modulator of insulin resistance in TLR 2 knockout mice. PLoS Biol. 2011; 9:e1001212. [PubMed: 22162948]
53. Jackman K, Kunz A, Iadecola C. Modeling focal cerebral ischemia in vivo. Methods Mol Biol. 2011; 793:195–209. [PubMed: 21913102]
54. Lin TN, He YY, Wu G, Khan M, Hsu CY. Effect of brain edema on infarct volume in a focal cerebral ischemia model in rats. Stroke. 1993; 24:117–121. [PubMed: 8418534]
55. Bouët V, et al. Sensorimotor and cognitive deficits after transient middle cerebral artery occlusion in the mouse. Exp Neurol. 2007; 203:555–567. [PubMed: 17067578]
56. Yagi S, Costanzo RM. Grafting the olfactory epithelium to the olfactory bulb. Am J Rhinol Allergy. 2009; 23:239–243. [PubMed: 19490794]
57. Jackman K, et al. Progranulin deficiency promotes post-ischemic blood-brain barrier disruption. J Neurosci. 2013; 33:19579–19589. [PubMed: 24336722]
58. Schloss PD, et al. Introducing mothur: open-source, platform-independent, community-supported software for describing and comparing microbial communities. Appl Environ Microbiol. 2009; 75:7537–7541. [PubMed: 19801464]
59. Buffie CG, et al. Precision microbiome reconstitution restores bile acid mediated resistance to Clostridium difficile. Nature. 2015; 517:205–208. [PubMed: 25337874]
60. Sheneman L, Evans J, Foster JA. Clearcut: a fast implementation of relaxed neighbor joining. Bioinformatics. 2006; 22:2823–2824. [PubMed: 16982706]
61. Garcia-Bonilla L, Racchumi G, murphy M, Anrather J, Iadecola C. Endothelial CD36 Contributes to Postischemic Brain Injury by Promoting Neutrophil Activation via CSF3. J Neurosci. 2015; 35:14783–14793. [PubMed: 26538649]
62. Pino PA, Cardona AE. Isolation of brain and spinal cord mononuclear cells using percoll gradients. J Vis Exp. 2011; doi: 10.3791/2348
63. Roederer M. Spectral compensation for flow cytometry: visualization artifacts, limitations, and caveats. Cytometry. 2001; 45:194–205. [PubMed: 11746088]

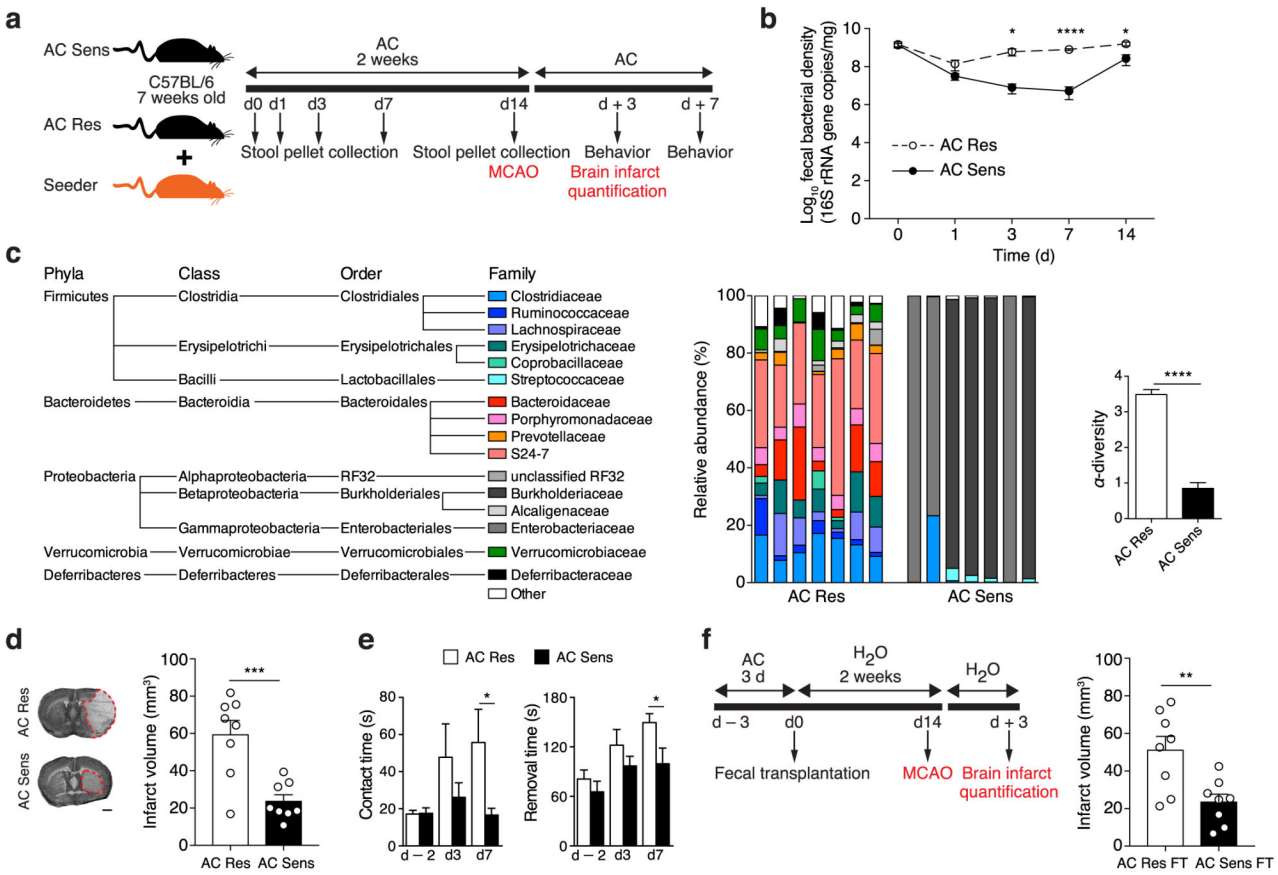

Figure 1.

Intestinal microbiota alteration protects from MCAO. (**a**) Experimental design of AC treatment in 7 weeks old C57BL/6 mice. AC Res mice, co-housed with AC Res seeder mice, and AC Sens flora mice received antibiotic via drinking water for 2 weeks. Stool collection time points are indicated. MCAO is induced after 2 weeks of AC and brain infarct volume is quantified 3 days later. Other groups of mice are assessed for sensorimotor function. (**b**) Fecal r16S DNA copy numbers in AC Res and AC Sens mice ($n = 5$ per group). (**c**) Left, family-level phylogenetic classification of fecal 16S rDNA gene frequencies from AC Res and AC Sens mice treated for 2 weeks. Each bar represents an individual animal. Right, graph depicts Shannon α-diversity index of grouped data ($n = 7$ per group). Only families with a frequency > 1% were included. (**d**) Infarct volume of AC Res and AC Sens mice 3 days post MCAO ($n = 8$ per group; bar, 1 mm). (**e**) Sensorimotor function in AC Res and AC Sens mice. Graphs show time to contact and remove the tape off the contralateral forepaw 2 days prior, 3 and 7 days after MCAO ($n = 11$ per group). (**f**) Left, fecal transplant (FT) experimental design. Mice are pulse-treated with AC for 3 days and gavaged with cecal contents of either AC Res or AC Sens donors. After 2 weeks on H_2O, FT recipient mice are subjected to MCAO and sacrificed 3 days after for infarct volume quantification. Right, graph shows infarct volumes ($n = 8$ per group). Columns represent mean ± s.e.m. $^*P < 0.05$, $^{**}P < 0.01$, $^{***}P < 0.001$ and $^{****}P < 0.0001$ (Student's *t*-test).

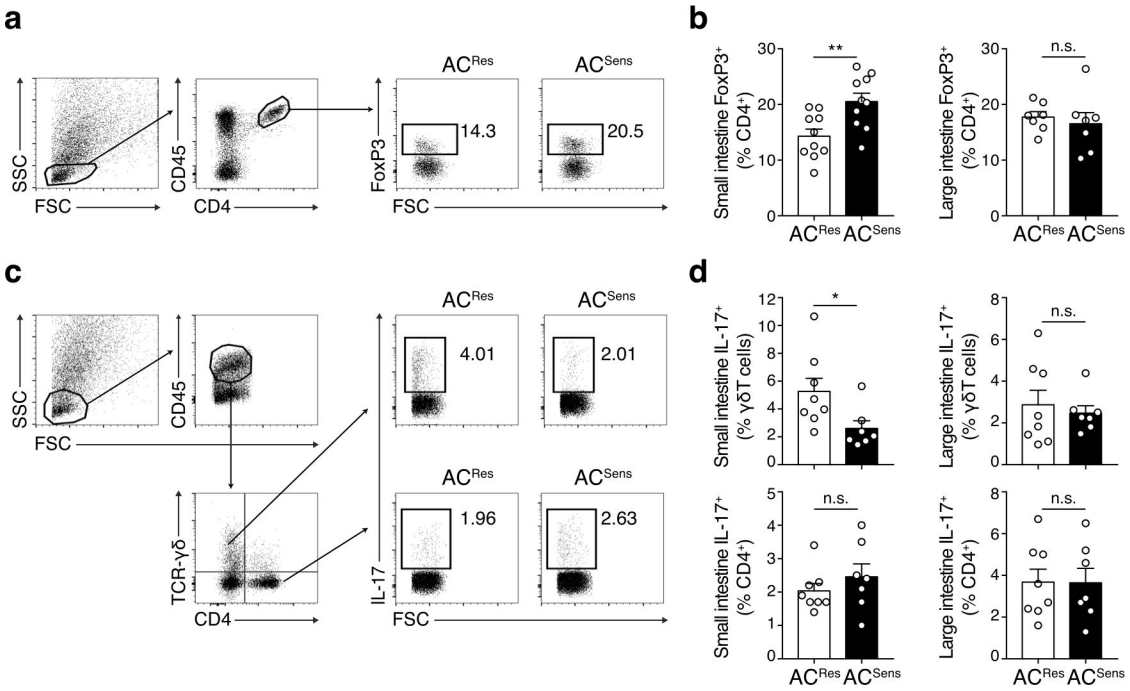

Figure 2.

Increased T_{reg} cells and reduced IL-17$^+$ γδ T cells in the small intestine of AC Sens mice. (**a**) Representative flow cytometry plots. Left, CD4 T cells identified in side scatter (SSC)/forward scatter (FSC) plots and CD45$^+$/CD4$^+$ expression. Mid panel, T_{reg} cells (CD45$^+$CD4$^+$FoxP3$^+$) in the LP of the small intestine of AC Res and AC Sens. Numbers represent events within the gate as percentage of CD4$^+$ cells. Right, graphs represent percentages of FoxP3$^+$ cells in the LP of the small intestine ($n = 10$ per group) and large intestine ($n = 7$ per group). (**b**) Flow cytometry analysis of IL-17 production in γδ T cells (CD45$^+$TCR-γδ$^+$CD4$^-$) and CD4$^+$ T cells (CD45$^+$TCR-γδ$^-$CD4$^+$) in the LP of the small intestine from AC Res and AC Sens mice after 2 weeks on antibiotics. The boxes in the center dot plots identify IL-17$^+$ cells and numbers represent IL-17$^+$ cells as a percentage of γδ T cells (first row) and CD4$^+$ cells (second row) in AC Res and AC Sens mice. The bar graphs on the right indicate percentages of IL-17-producing cells in the LP of the small and large intestine (AC Res, $n = 8$ and AC Sens, $n = 7$). Columns represent mean ± s.e.m. *$P <$ 0.05, **$P < 0.01$; n.s., not significant (Student's t-test).

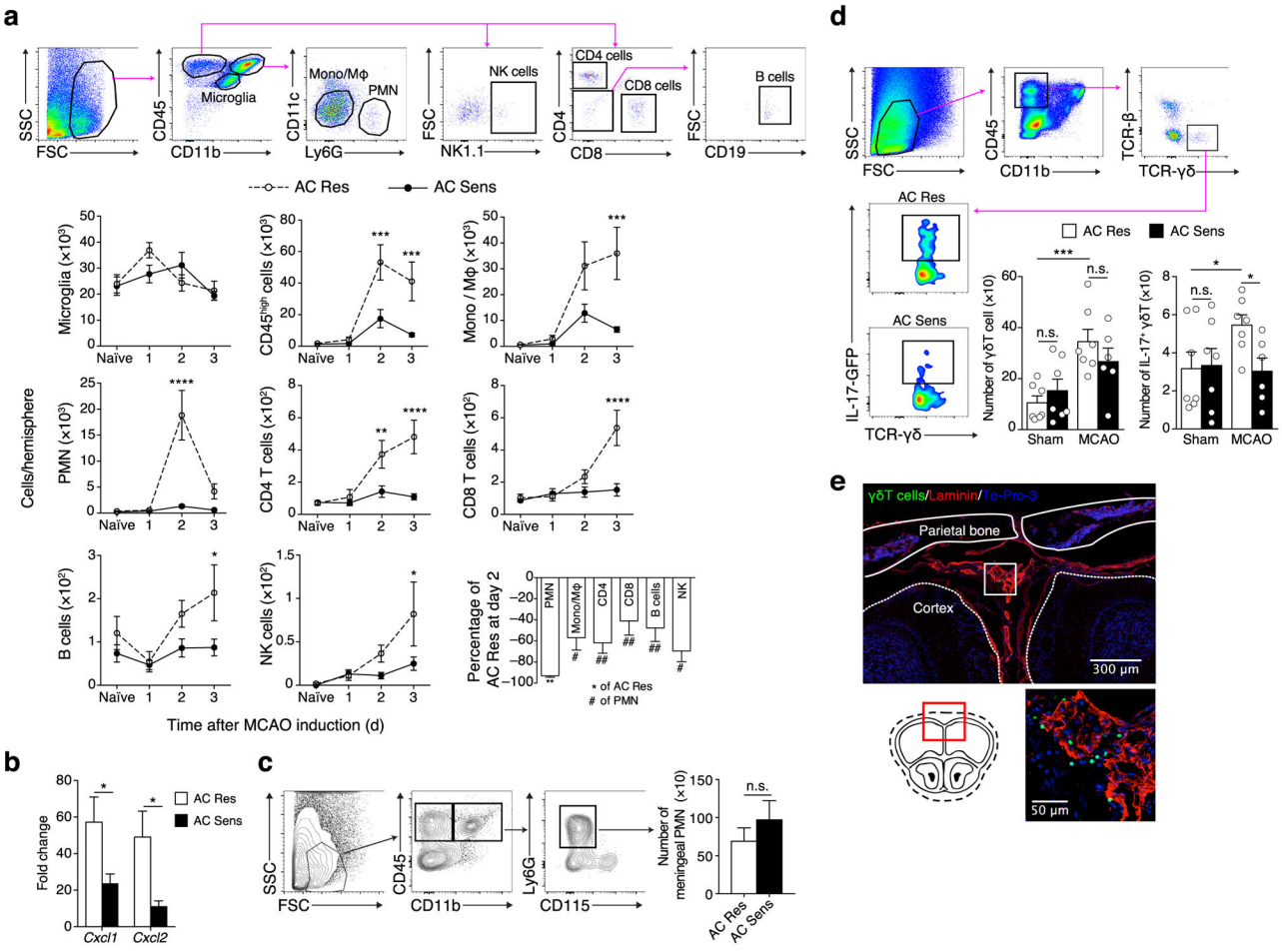

Figure 3.

Accumulation of IL-17$^+$ γδ T cells at the meninges is associated with increased infarct size. (**a**) Flow cytometric gating strategy of brain microglia (CD45^{int}CD11b^{int}) and infiltrating leukocytes (CD45^{high}) including monocytes/macrophages (Mono/MΦ; CD11b$^+$Ly6G$^-$CD11c$^-$), neutrophils (PMN; CD11b$^+$Ly6G$^+$CD11c$^-$), CD4$^+$ T cells (CD11b$^-$CD4$^+$CD8$^-$), CD8$^+$ T cells (CD11b$^-$CD8$^+$CD4$^-$), B cells (CD11b$^-$CD4$^-$CD8$^-$CD19$^+$) and natural killer cells (NK; CD11b$^-$NK1.1$^+$) in AC Res and AC Sens naïve mice and days 1, 2 and 3 after MCAO. Graphs represent absolute number of cells in the ischemic hemisphere (n = 5–9 per group, Supplementary Table 3). Bottom right graph, percentage of leukocyte reduction 2 days after reperfusion (n = 8–9 per group, Supplementary Table 3). Values are mean ± s.e.m. $^{**}P < 0.01$ versus AC Res; $^{\#}P < 0.05$ and $^{\#\#}P < 0.01$ versus neutrophils (Student's t-test). (**b**) *Cxcl1* and *Cxcl2* mRNA expression in brains of AC Res and AC Sens mice 1 d after MCAO (n = 10 per group). Values are fold change over brain from naïve mice. (**c**) Flow cytometric gating strategy of meningeal PMN in AC Res and AC Sens mice 1 d after MCAO. Graph represents PMN cell number quantification in the meninges (n = 9 per group). (**d**) Flow cytometry analysis of meningeal IL-17$^+$ γδ T cells (CD45^{high}CD11b$^-$TCR-β$^-$TCR-γδ$^+$IL-17$^+$-GFP) of AC Res and AC Sens IL-17-eGFP mice 16 h after MCAO. Left graph represents the total number of γδ T cells and

right graph, total number of IL-17$^+$ γδ T cells in the meninges of AC Res and AC Sens mice subjected to sham surgery (n = 7 per group) and after MCAO (AC Res, n = 7; AC Sens, n = 6). Each data point (n) is derived by pooling 2 hemispheres. (**e**) Representative photomicrographs of meningeal γδ T cells (green; TCR-γδ-GFP$^+$), laminin (red) and cell nuclei (blue, To-Pro-3) 16 h after MCAO. Coronal section is taken at Bregma + 3 mm. Columns and line plots represent mean ± s.e.m. *P < 0.05, **P < 0.01, ***P < 0.001 and ****P < 0.0001; n.s., not significant (Student's t-test)

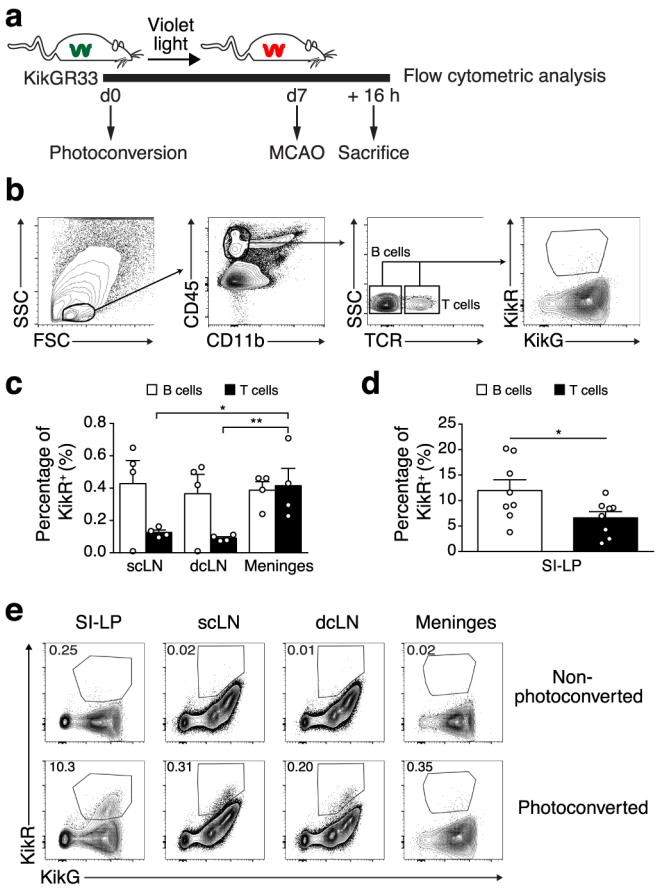

Figure 4.

Migration of intestinal T cells to the meninges after ischemic brain injury. (**a**) Photoconversion of the distal part of the small intestine is induced in KikGR mice 7 days prior MCAO using violet light. Photoconverted cells ($KikR^+$ cells) are analyzed in different tissues by flow cytometry 16 h after MCAO. (**b**) Flow cytometry gating strategy in photoconverted KikGR mice. T cells ($CD45^+CD11b^-TCR^+$) and B cells ($CD45^+CD11b^-TCR\text{-}\beta^-TCR\text{-}\gamma\delta^-$) express the red variant of the protein ($KikR^+$) in the meninges 16 h after MCAO. (**c**) Percentage of photoconverted cells ($KikR^+$) of total B or T cells in superficial cervical lymph nodes (scLN; $n = 4$), deep cervical lymph nodes (dcLN; $n = 4$) and meninges ($n = 4$). One data point is derived from 3 pooled animals. Columns represent mean ± s.e.m. $^*P < 0.05$ and $^{**}P < 0.01$ (one way-ANOVA and Tukey's test). (**d**) Proportion of $KikR^+$ B and T cells in the LP of the small intestine (SI-LP; $n = 8$). One data point is derived from one animal. Columns represent mean ± s.e.m. $^*P < 0.05$ (Student's *t*-test). (**e**) Analysis of photoconverted $CD45^{high}CD11b^-$ cells in different organs, showing the different signal from a non-photoconverted and a photoconverted mouse 16 h after ischemia. The gates in the dot plots identify $KikR^+$ cells, and the numbers are the percentage of $KikR^+$ cells of pan-lymphocytes ($CD45^{high}CD11b^-$).

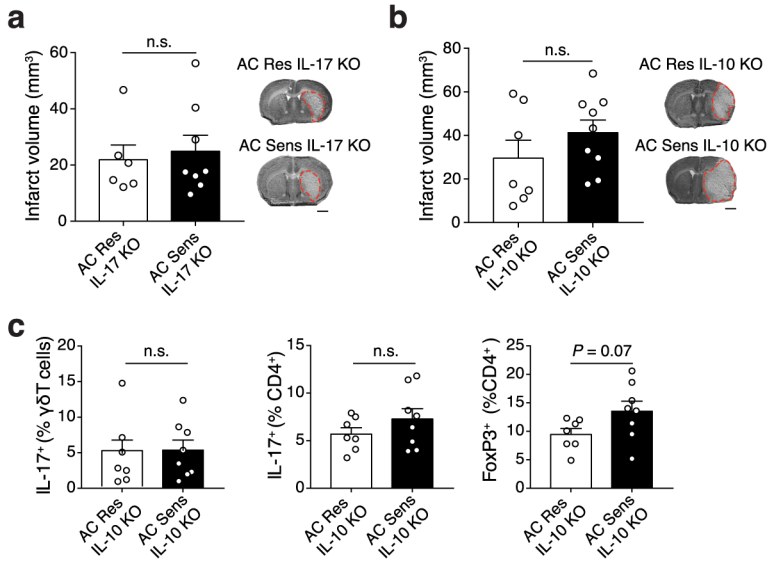

Figure 5.

Neuroprotection conferred by intestinal dysbiosis requires a reduction in intestinal IL-17$^+$ γδ T cells. (**a**) Infarct volume in AC Res (n = 6) and AC Sens (n = 8) IL-17 KO mice as measured by Nissl staining of coronal brain sections 3 days after MCAO (bar, 1 mm). (**b**) Infarct volume of AC Res (n = 7) and AC Sens (n = 9) IL-10 KO mice on day 3 post MCAO. Representative coronal sections with Nissl staining are shown (bar, 1 mm). (**c**) The graphs represent the percentage of IL-17$^+$ γδ T, T_H17 and FoxP3$^+$ cells, respectively, in the LP of the small intestine from AC Res (n = 7) and AC Sens (n = 8) IL-10 KO mice after 2 weeks on antibiotic treatment as measured by flow cytometry. Columns represent mean ± s.e.m.; n.s., not significant (Student's t-test).

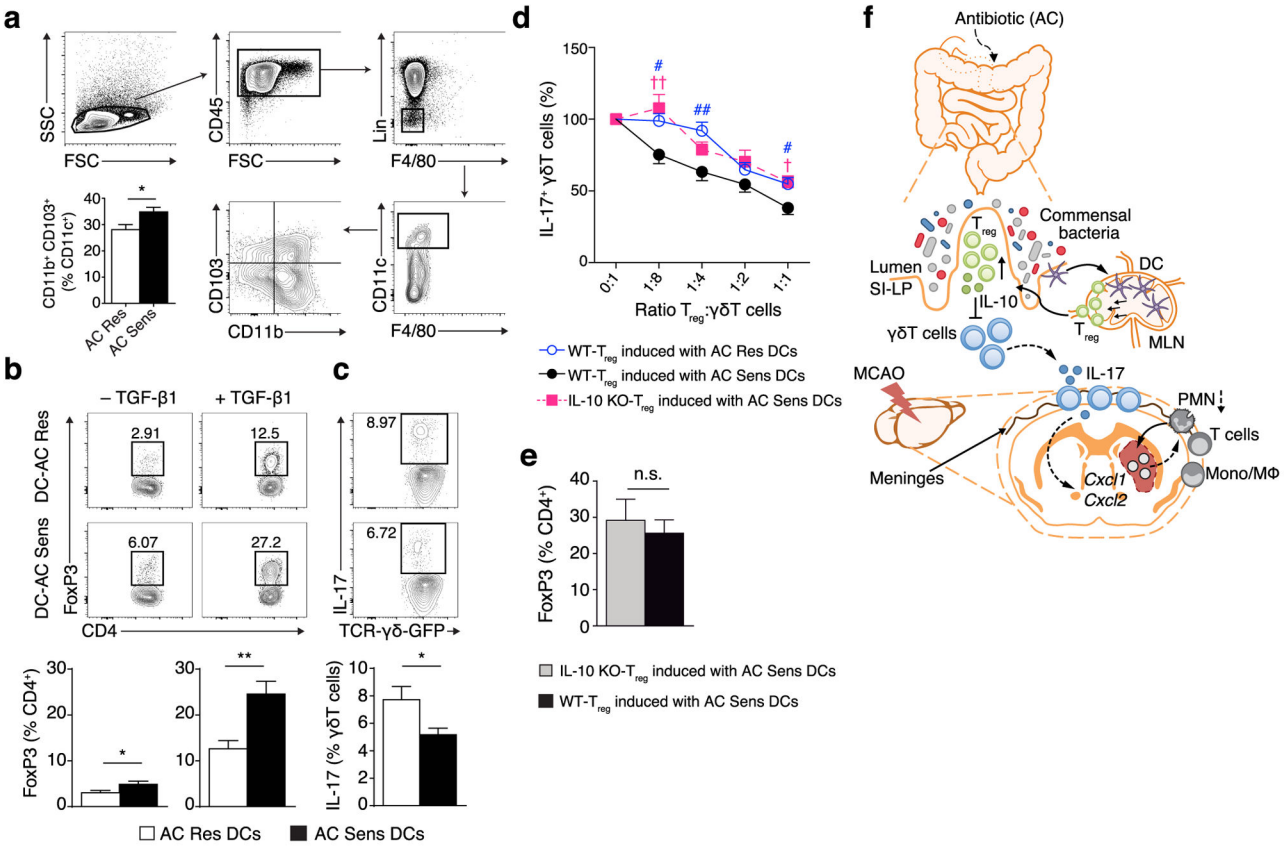

Figure 6.

DCs from AC Sens originate in the intestine, induce T_{reg} cells and downregulate IL-17$^+$ γδ T cells *in vitro*. (**a**) Flow cytometry analysis of DCs (CD45^{high}CD11c$^+$F4/80$^-$Lin$^-$; Lin = B220$^+$CD3ε$^+$) isolated from mLN of AC Sens and AC Res mice. Graph represents percentage of CD11b$^+$CD103$^+$ subpopulations in CD11c$^+$ cells (n = 12 per group). (**b**) Flow cytometry analyzing T_{reg} cells (CD4$^+$FoxP3$^+$) co-cultured with DCs from AC Res or AC Sens mice in absence (n = 7 per group, left plots) or presence of TGF-β1 (n = 5 per group, right plots). Numbers in the dot plots are percentages of T_{reg} cells of total CD4+ cells. Graphs represent percentage of T_{reg} (n = 5 per group). (**c**) Flow cytometric analysis of IL-17 expression in γδ T cells co-cultured with DCs from AC Res or AC Sens mice (n = 9 per group). Gates in the dot plots identify IL-17$^+$ γδ T cells, and the numbers are the percentage of IL-17$^+$ cells of total γδ T cells. Graph represents percentage IL-17$^+$ γδ T (n = 7 per group). (**d**) Suppression of IL-17$^+$ γδ T cells by co-culture with T_{reg} cells generated *in vitro* by incubating WT or IL-10 KO CD4+ cells with DC from AC Res or AC Sens mice. (WT n = 11, IL-10 KO n = 9 per data point), Supplementary Table 4). (**e**) Percentage of T_{reg} cells induced by DCs from AC Sens in WT and IL-10 KO mice (n = 6 per group). Columns and line plots represent mean ± s.e.m. *P < 0.05, **P < 0.01; n.s., not significant (Student's t-test). † and #P < 0.05, †† and ##P < 0.01 (one-way ANOVA). (**f**) Proposed mechanism of protection from ischemic brain injury induced by intestinal microbial dysbiosis. Two weeks of AC results in microbial dysbiosis. Mesenteric lymph node DCs that originate in the small intestine induce T_{reg} cells. After homing to the gut, IL-10 secreting T_{reg} cells suppress

IL-17$^+$ γδ T differentiation. Effector T cells traffic from the intestine to the meninges where a reduction in IL-17$^+$ γδ T cells decreases post-ischemic chemokine expression and leukocyte infiltration improving outcome after brain ischemia.